https://doi.org/10.31436/iiumej.v20i2.1119

EXPERIMENTAL AND FINITE ELEMENT ANALYSIS OF SOLVENT CAST POLY(LACTIC ACID) THIN FILM BLENDS

SHARIFAH IMIHEZRI SYED SHAHARUDDIN*, ABDUL RAHMAN MUKHTAR, NUR ATIQAH MOHD AKHIR, NORHASHIMAH SHAFFIAR, MAIZATULNISA OTHMAN

Department of Manufacturing and Materials Engineering,
Kulliyyah of Engineering, International Islamic University Malaysia,
Kuala Lumpur, Malaysia.

Corresponding author: shaimihezri@iium.edu.my

(Received: 21th March 2019; Accepted: 14th July 2019; Published on-line:2nd December 2019)

ABSTRACT: A combined experimental and finite element analysis (FEA) investigation was performed to study the effect of incorporating poly(propylene carbonate)(PPC) and curcumin on the mechanical properties of poly(lactic acid) (PLA). In addition, the chemical interaction and morphological changes brought upon by each subsequent additive were also observed. The addition of PPC at 30 wt% into PLA causes a decrease in strength and modulus by 51% and 68% respectively whilst inducing higher elongation by 74%. The resultant decrease in strength and modulus of the PLA/PPC blend was recovered by adding a low weight percentage (1 wt%) of curcumin. The images of the fractured surfaces via scanning electron microscope (SEM) revealed the brittle-ductile-brittle progression of PLA due to the addition of PPC and curcumin which corroborates the findings from the tensile test. Fourier-transform infrared spectroscopy (FTIR) revealed that the addition of PPC by 30 wt % resulted in chemical interaction between the carbonyl groups of PLA and PPC as the C=O peak of PLA slightly shifted to a lower wavenumber. The presence of curcumin peaks however was found to be difficult to be identified in the PLA/PPC/curcumin blend. The simulated results for the stress-strain profile using FEA agreed well with the experimental tensile test profile with a relatively low percentage error of less than 6%. Therefore, it was concluded that for these compositions, the developed model can be used for further simulation works to design biomedical devices.

ABSTRAK: Gabungan penyelidikan secara eksperimen dan analisis unsur terhad (FEA) telah dijalankan bagi mengkaji kesan campuran poli (propilen karbonat) (PPC) dan kurkumin pada sifat mekanikal poli (asid laktik) (PLA). Tambahan, interaksi kimia dan perubahan morfologi pada setiap penambahan berikutnya turut diperhatikan. Penambahan PPC pada 30 wt% ke dalam PLA menyebabkan pengurangan pada tenaga dan modulus sebanyak 51% dan 68% masing-masing sementara menyebabkan kenaikan pemanjangan sebanyak 74%. Hasil pengurangan pada tenaga dan modulus campuran PLA/PPC diseimbangkan dengan mencampurkan peratus kurkumin kurang berat (1 wt%). Melalui mikroskop imbasan elektron (SEM), didapati imej permukaan retak menunjukkan PLA berturutan rapuh-mulur-rapuh disebabkan penambahan PPC dan kurkumin di mana ianya menyokong dapatan kajian ini melalui ujian kekuatan tegangan. Spektroskopi Inframerah Jelmaan Fourier (FTIR) menunjukkan dengan penambahan PPC sebanyak 30 wt %, interaksi kimia antara kumpulan karbonil PLA dan PPC pada puncak C=O PLA telah berubah sedikit kepada nombor gelombang lebih kecil. Walau bagaimanapun, kehadiran puncak kurkumin adalah sukar dikenal pasti dalam campuran PLA/PPC/kurkumin. Dapatan hasil simulasi pada profil strain-tekanan menggunakan FEA adalah sama dengan ujian kekuatan tegangan dengan peratus ralat yang agak rendah iaitu kurang daripada 6%.

Oleh itu, komposisi model yang dibangunkan ini adalah sesuai bagi meneruskan kerja-kerja simulasi iaitu bagi mereka bentuk alat biomedikal.

KEYWORDS: *PLA; PPC; curcumin; tensile; FEA*

1. INTRODUCTION

Poly(lactic acid) (PLA), recently, has been the main thermoplastic polymer candidate for applications that require tailored biodegradability feature such as in the biomedical as well as food and packaging industry [1]. The biomedical application of PLA is due to its ability to fulfil complex requirements in terms of biodegradability, and thermoplastic processability [2, 3]. In comparison to other traditionally studied biodegradable polymers, PLA is able to provide excellent features at low cost [4]. PLA offers good thermal processability, thus, the polymer can be processed via various techniques such as injection moulding, film extrusion, blow moulding and fiber spinning. Despite the polymer's copious advantages, the application of PLA has been restricted to a certain extent due to its inherent brittleness, hydrophobicity, poor heat resistance and poor degradation rate [5,6]. Specifically, one of the main drawbacks of PLA for biomedical application is attributed to its high brittleness [7], since it reduces the flexibility and plasticity [8] of the polymer. The brittleness of PLA is a result of the formation of large spherulites due to its slow crystallization rates [9]. A simple and efficient method to modify the flexibility, strength, processability, and impact toughness of PLA is by blending with various plasticizers such as poly(propylene carbonate) (PPC) [10,11], polyethylene glycol (PEG) [12,7], glucosemonoesters , poly(vinyl acetate) (PVAc) [13], and partial fatty acid esters.

The biodegradable poly(propylene carbonate) (PPC) is synthesized from copolymerization of renewable CO_2 and propylene oxide (PO) and is typically amorphous [14]. PPC has a chemical structure akin to that of PLA as shown in Fig. 1. The polymer offers good mechanical property, in particular ductility that could be used to improve the toughness of PLA [11]. In comparison to PLA, PPC has a relatively low glass transition temperature (around 35 °C) due to the lack of a strong polar group in its chain, therefore enabling the PPC chain segment to move easily [15]. Hence, PPC displays a very flexible structure. The polymer‘s elongation at break is nearly 330%, which is at least five-fold greater in comparison to other polyesters [16].

(a) (b)

Fig. 1: The chemical structure of (a) Polylactic acid, PLA and (b) Poly(propylene carbonate), PPC [11].

Curcumin, an orange-yellow crystalline powder with a chemical structure shown in Fig. 2 is prepared from solvent extraction followed by purification of ground rhizomes of turmeric [17]. Curcumin is commonly used in various applications such as foods and cosmetics. Due to its medicinal properties, there is a high tendency for curcumin to be used in medical applications for antibacterial, antitumor, and antioxidant purposes [18-21]. The bioactivities of curcumin such as anti-cell adhesion and motility, anti-angiogenesis and anti-microbe properties have been elucidated in *in vivo*/*in vitro* studies [22]**.** Various curcumin/polymer blends have been electrospun into nanoscale fiber scaffolds or mats [21,

23]. Several studies of wounded animals treated with PLA/curcumin nanofiber mats have been noticed to undergo improved wound closure rates [24, 25]

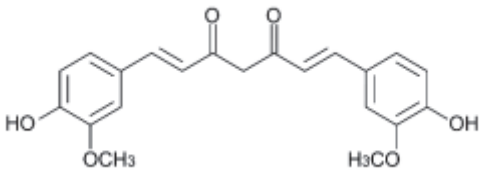

Fig. 2: The chemical structure of curcumin [26].

Thin films often experience very high stresses during service which leads to distortion or deformation [27]. Finite element analysis (FEA) provides insight in identifying critical locations of the device (high stress/strain regions), reduces design iterations/optimization, and reduces the need for bench-top testing; thereby reducing the cycle time during product development [28]. FEA has been used not only to model the mechanical properties [29,30] but also degradation performances [31,32] of various materials. Previously, flat tension specimens of various ceramic matrix composites and monolithic ceramics have been studied via FEA for creep performance [33]. This work was prompted by the scarcity of FEA study on flat thin films subjected to uniaxial tensile tests. The motivation for this study is twofold: first, to study the effect of PPC and curcumin addition on PLA upon its structural, morphological and mechanical properties, and second, to simulate the mechanical effect of PPC and curcumin addition in the elastic and plastic region using FEA (ABAQUS).

2. METHODOLOGY

2.1 Sample Preparation

PLA (IngeoTM Biopolymer 3052D) was obtained from Nature-works (USA) whilst PPC (QPAC 40) was sourced from Empower Materials (Malaysia). Analytical grade chloroform (R&M Chemicals, United Kingdom) was used as solvent. The curcumin (Live-well^{TM}) used in this study was manufactured by Pahang Pharmacy Sdn. Bhd. (Malaysia). Both PLA and PPC pellets were dried at 70 °C and 40 °C respectively for 2 hrs in an oven prior to being dissolved in chloroform. Subsequently, PLA, PPC and curcumin were prepared at different weight % ratios (PLA:PPC -100:0, PLA:PPC - 70:30 and PLA:PPC:curcumin; 69:30:1). Both PLA and PPC were dissolved in chloroform at the ratio of 1:10. Upon complete dissolution, curcumin was then added and stirred for 1 hour. Each blend was then poured into a Teflon covered container and was left to dry for 24 hours at ambient temperature.

2.2 FTIR Analysis

Identification of the functional groups of the PLA and PLA/PPC blends were obtained by using Tensor 27 FTIR Spectrometer (Bruker, USA). The spectra were collected within 4000 – 600 cm^{-1} region with a resolution of 4 cm^{-1} and 16 scans.

2.3 Morphological Observation

The surface of the fractured tensile test specimens were sputtered with palladium using a Quorum SC7620 Sputter Coater in order to make the surface conductive prior to SEM analysis. The resulting surfaces were then observed via InTouch Scope JSM-IT100 (JEOL).

2.4 Tensile Test

https://doi.org/10.31436/iiumej.v20i2.1119

The FEA simulations for the studied polymers were based on the stress-strain response of the materials conducted according to ASTM D882. Thin films were cut according to the following dimensions of 50 mm × 10 mm × 0.80 mm with an extra 10 mm at both ends for clamping purposes as shown in Fig. 3. The grey tabs in this figure represent the glued cardboard strips of the same size, by which the sample is clamped between machine grips. Tensile tests were performed using a Shimadzu Universal Tensile Machine (AGS-10K NXD) at a crosshead speed of 20 min/mm with a load cell of 5 kN. The average and standard deviation of the mechanical properties were calculated from the load-elongation curve based on 5 samples.

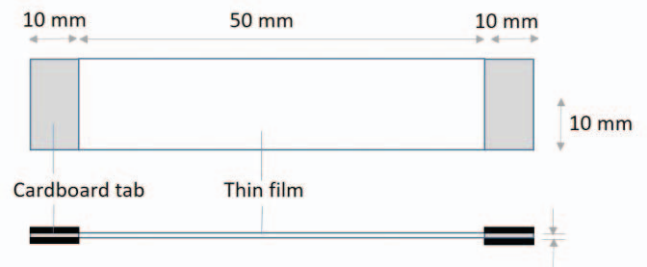

Fig. 3: Preparation of test specimen for tensile test.

2.5 Simulation Model

The FE model of the thin films were developed using Abaqus software. The 3D model was discretized into a structured element mesh using 3D linear hexahedral elements (C3D8R) which resulted in total mesh and node values of 1562 and 700 respectively for all samples. A schematic representation of the tensile specimen as well as the boundary condition inflicted on the sample is shown in Fig. 4.

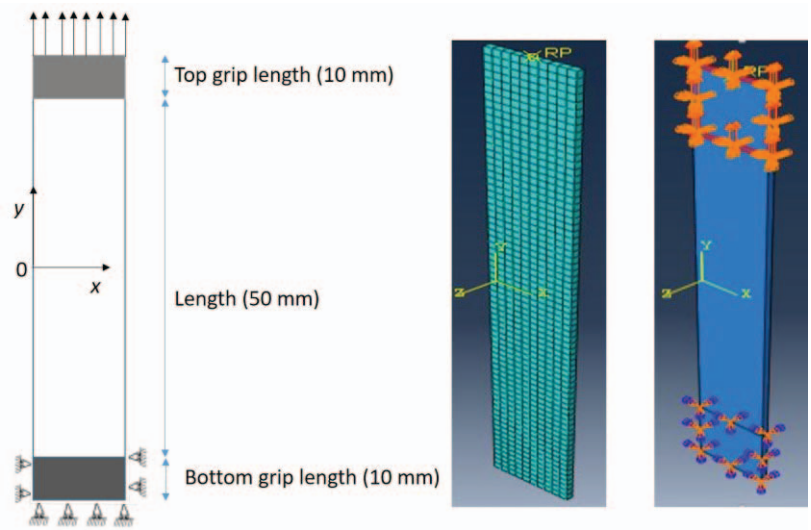

(a) (b) (c)

Fig. 4: (a) Schematic representation of the specimen geometry (b) Finite element mesh using 3D linear hexahedral elements (C3D8R) (c) boundary conditions for the simulation of the tensile test.

In the actual tensile test, each specimen was clamped and displaced using hydraulic rigid grips. The additional length of 10 mm at each end of the sample functions as a grip length in which the top grip length will be displaced upward by the load cell whilst the bottom grip

length would be stationary. In order to replicate the experimental tensile test, the boundary and loading conditions were translated as follows [34]; the top grip length (10 mm) and sample test length (50 mm) were kept as fixed in all directions but unconstrained in the direction of the load applied. The top grip was loaded with an upward load of 5 kN. Meanwhile, the bottom grip length had no degree of freedom. The average thickness of each sample was 0.8 mm. The constitutive material data for the elastic model in the simulation were defined by the experimental elastic modulus whilst Poisson's ratio was obtained from the literature [35] as shown in Table 1. The plasticity model was included in the FEA by defining the region of yield stress and corresponding plastic strain that were obtained from the experiment. There were no purposefully designed geometrical flaws such as notches or necking in the simulation model that would trigger localization of the specimen at any desired region.

Table 1: Material properties used for the FEA simulation element

Composition (wt%)	Young's modulus (MPa)	Yield strength (MPa)	Poisson's ratio
Neat PLA	936	8.4	0.36
PLA / PLC (70:30 wt%)	156	3.5	0.36
PLA / PPC / curcumin (69:30/1 wt%)	771	11.7	0.36

3. RESULTS AND DISCUSSION

3.1 FTIR

Figure 5 shows the FTIR spectra of neat PLA, PPC, and curcumin as well as their blends. The FTIR detects the chemical interaction and compatibility between the molecular chains of different polymer blends by the shift and broadening of the absorption band [36]. The neat PLA spectra shows characteristic stretching frequencies for C=O, $-CH_3$ asymmetric, $-CH_3$ symmetric, and C–O, at 1752 cm^{-1}, 2995 cm^{-1}, 2947 cm^{-1} and 1085 cm^{-1}, respectively. The PPC spectra shows the typical characteristic peaks at 2920 cm^{-1}, 1746 cm^{-1}, and 1235 cm^{-1} attributed to C-H bond stretching vibration, C=O bond stretching vibration and C-O stretching respectively. In the 3700 – 3100 cm^{-1} region, the absorption of neat PPC and PLA is not identified due to the rarity of terminal O-H groups.

The PLA/PPC spectra in the high wavenumber region, (3100-2800 cm^{-1}), relates to the -CH- stretching vibration, which shows similar absorption peaks as pristine PLA. Ma et al. [38] observed that the stretching vibration may shift with higher PPC loading dueto intermolecular interaction between C-H and O-C- or between C-H and O=C-. PLA is made from lactic acid and forms rich carbon chains that serve as the main functional group (C=O groups). The functional group is detectable at the frequency region of 1740-1750 cm^{-1} (denoted as 'A') [37]. The addition of 30 wt % PPC causes the C=O peak of PLA at 1752 $cm^{-1}$to slightly shift to a lower wavenumber cm^{-1} (by 3 cm^{-1}). Therefore, implying that the carbonyl groups may have taken part in the interaction between PLA and PPC. Such interaction could be between C-H…O=C-, C=O…O=C or C=O…O-C dipole-dipole interaction [38]. A more significant wavenumber shift of up to 11 cm^{-1} has been observed with higher PPC loading [38]. It was noted that there is no significant peak shift in the C-H bending ('B' region) as well as the C-O stretching vibration ('C' region). It was deduced that despite the similar chemical nature of PLA and PPC, the addition of 30 wt% of PPC only resulted in chemical interaction between the carbonyl groups of these polymers.

https://doi.org/10.31436/iiumej.v20i2.1119

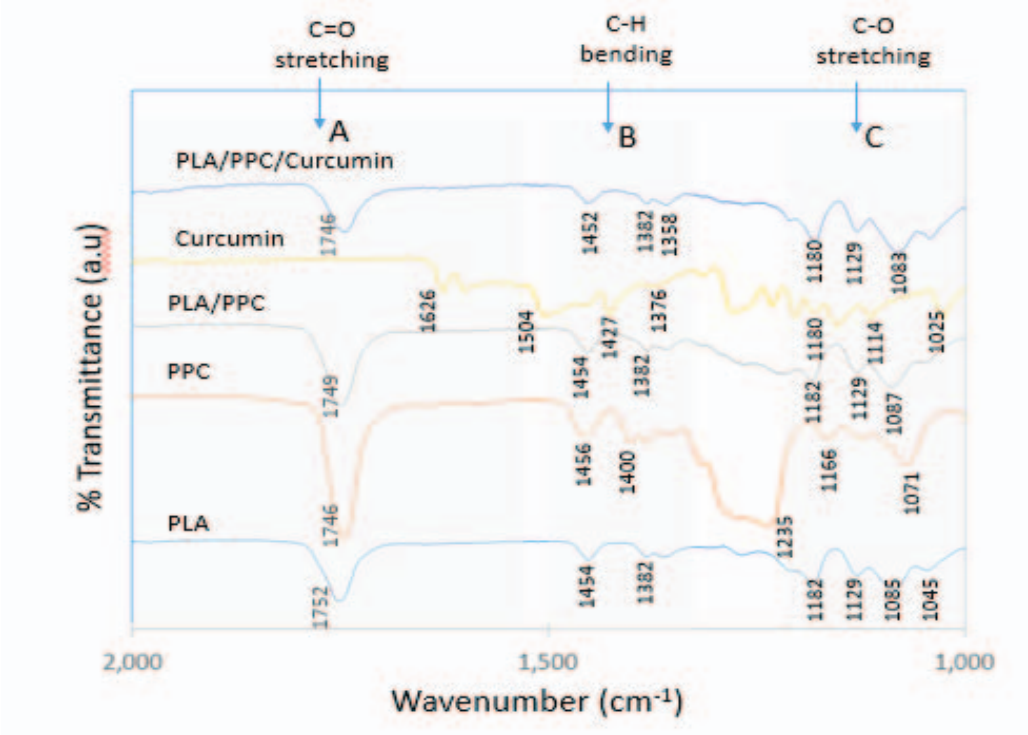

Fig. 5: Fourier transform infrared (FTIR) spectra of PLA, PPC, PLA/PPC, and PLA/PPC/curcumin blends.

Curcumin can be distinguished by its phenolic O-H stretching band at 3508 cm^{-1} [26, 39]. Other significant curcumin bands are the aromatic C-C band (1602 cm^{-1}), olefinic C-H (1428 cm^{-1}), asymmetric C-O-C (1026 cm^{-1}) and phenolic C-O (1276 cm^{-1}) [40, 39]. These significant peaks are found to be comparable and appear at 3507 cm^{-1}, 1601 cm^{-1}, 1428 cm^{-1}, 1026 cm^{-1} and 1274 cm^{-1} respectively. A sharp common peak at 1180 cm^{-1}, assigned as phenolic C-O is observed in both curcumin and PLA/PPC/curcumin, hence confirming the presence of curcumin in the blend. Apart from the C-O phenolic peak, the lack of presence of other curcumin peaks observed in the PLA/PPC/curcumin trace suggests that these curcumin peaks were either eclipsed by the more generous peaks of PLA at that wavenumber range due to the higher weight % of PLA [41]. The FTIR samples for PLA/PPC/curcumin were performed twice to confirm such a scenario. Previously, Chen et al. [42] reported that curcumin loading below 5% would not give any chemical reaction with PLA.

3.2 Tensile Test

The tensile test was conducted to investigate the mechanical effect of adding 30 wt% of PPC and 1% of curcumin at the expense of PLA. Figure 6 illustrates that the neat PLA curve behaves linearly in the low strain, then starts to plastically deform in the region of 3% strain. The strain at break of neat PLA in this study is 11.7% and is higher than the PLA thin films studied by Yao et al. [10]. Aside from the grade of PLA used, the difference in sample thickness, as well as testing speed [13], it is postulated that the strain value in this study may have also been affected by the sample preparation technique since the thin films in their study [10] were prepared by melt compounding.

https://doi.org/10.31436/iiumej.v20i2.1119

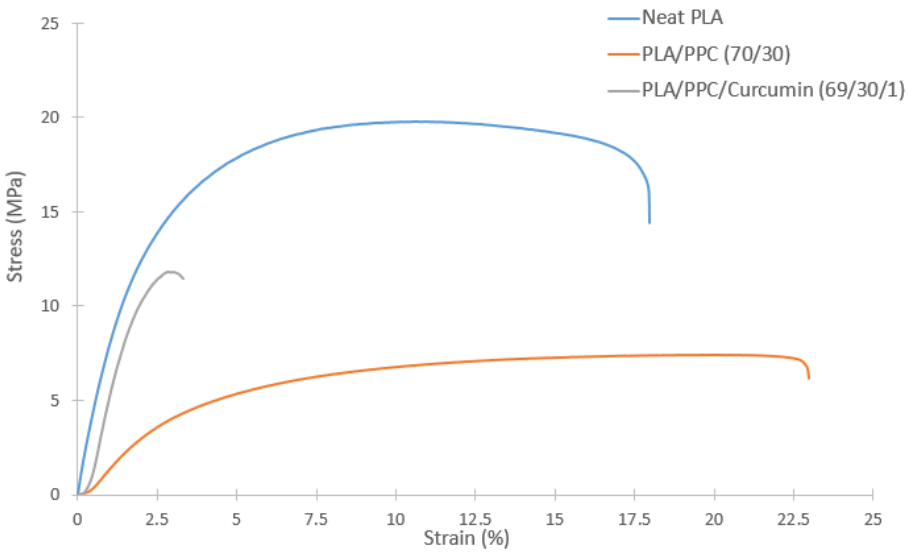

Fig. 6: Stress-strain curves for neat PLA, PLA/PPC, and PLA/PPC/curcumin.

Studies on PLA/PPC blends by Zao et al. [43] and Yu et al. [44] suggest that the addition of 30 wt% of PPC creates the optimum blend after considering the resulting elongation and flexural and impact strength properties. In this study, the addition of 30 wt % of PPC into PLA causes a decrease of strength and modulus by 51% and 68% respectively (Table 2). The trend of decreasing tensile strength and Young's modulus upon blending of PPC into PLA is well documented. Studies by Ma et al. [38] and Zou et al. [43] show a decreasing trend in strength as well as of modulus with further loading of PPC. It is also seen that PPC contributes to the elastic component. As a result, a higher strain at break by 74% was achieved in the PLA/PPC blend in this study. Such an increase in strain value is manifested from the weak molecular chain interaction and the presence of plenty weak flexible, polar C–O–C bonds in the backbone structure of PPC [15, 43]. Sun et al. [45] suggested that the transformation of PLA from brittle to ductile nature indicates a good compatibility between PLA and PPC as evidenced by the chemical interaction found in FTIR.

Table 2: Mechanical properties of neat PLA, PLA/PPC and PLA/PPC/curcumin

Properties	Neat PLA	PLA / PPC	PLA/ PPC/Curcumin
Modulus (MPa)	481.3 ± 145.1	155.4 ± 26.9	726.7 ± 62.4
Strength (MPa)	15.3 ± 2.8	7.4 ± 0.3	11.0 ± 1.1
Strain at break (%)	11.7 ± 3.3	20.4 ± 1.4	2.4 ± 0.7

The addition of 1 wt % of curcumin significantly improves the strength and modulus of PLA/PPC, hence suggesting that the curcumin particles act as reinforcement filler. The presence of curcumin creates resistance that reduces the mobility of internal PLA/PPC structures and resulted in an enhanced stiffness property. However, the inclusion of filler also increases the polymer blends' brittleness characteristics [46]. As seen here, when the PLA/PPC/curcumin was subjected to tensile-mode deformation, the samples failed at very low tensile strain. The composition of curcumin was restricted to only 1 wt% in this study since previous study by the author [47] has shown a decreasing trend in strength with further curcumin additions. An obvious decrease in the tensile strength at higher filler content is

likely to occur as the filler-matrix interaction is replaced by the contact between particles as well as filler agglomeration [46, 48].

3.3 Surface Morphology

The photographs of the dried polymer blend films are shown in Fig. 7. The addition of PPC into PLA increases opacity whilst the addition of curcumin imparts yellowish hue due to the bioactive yellow pigment from curcumin with the following structure; 1,7-bis(4-hydroxy-3-methoxyphenyl)-1,6-heptadiene-3,5-dione.

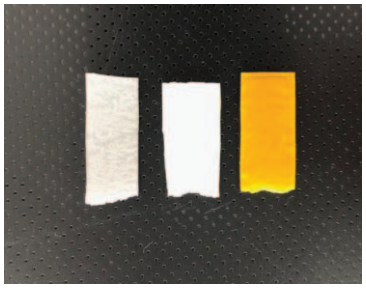

Fig. 7: From left to right, fractured tensile test specimens of PLA, PLA/PPC, and PLA/PPC/curcumin.

The morphological structure of the PLA blend was examined via SEM, and the results are shown in Fig. 8. The SEM image of neat PLA exhibited the fractured surface that occurs at different layers and at different parts of the sample. Similar surface topography was observed from other studies [13, 49] that confirms the brittle nature of PLA. The blending of PPC into PLA creates a surface fracture that is much smoother with no visible aggregation. Such effect signals good dispersion and homogeneity in the blended films. The transition of the PLA and PLA/PPC samples from rough to smooth surface are in agreement with the observations made from the mechanical properties, in which the neat PLA progresses from a brittle to a ductile nature with the decrease in stiffness and an increase in strain values. In comparison, the addition of curcumin induces a much rougher fractured surface with a phase-separated morphology. It was observed that the dispersed curcumin particles created almost spherical and empty voids at the fractured surface. The change in the fractured surface of PLA/PPC blend from smooth to rough correlates to the effect of filler particle addition that changes the PLA/PPC from being ductile to a more brittle nature [46].

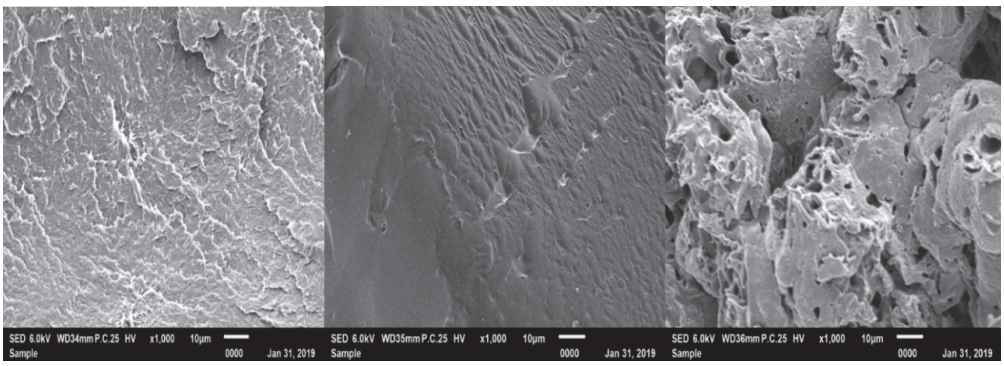

Fig. 8: SEM micrographs at 1000x magnification of the surfaces of the fractured (a) neat PLA (b) PLA/PPC (c) PLA/PPC/curcumin films subjected to uniaxial tensile stress.

3.4 Finite Element Analysis of the Tensile Test

The results from FE simulations are compared to the experimental data in Fig. 9 - Fig. 11. The graphs obtained show that the simulated stress-strain behaviour (overall shape) in the elastic and plastic region are in excellent agreement with the experimental data for all compositions studied. The damage criterion model was not implemented in this FEA model, hence the simulation and experimental work are comparable up to the ultimate tensile strength (maximum stress) only. The convergence between the simulation and experimental results near the maximum stress value indicates the reliability of the model since the maximum stress value is generally used as a criteria in design. The accuracy of the experimental and simulated model was obtained by comparing the integrated area beneath the stress-strain curves. Simulation performed using Abaqus FEA models described accurate results with a relatively low percentage error of 1% for both PLA as well as PLA/PPC and 6% for PLA/PPC/curcumin.

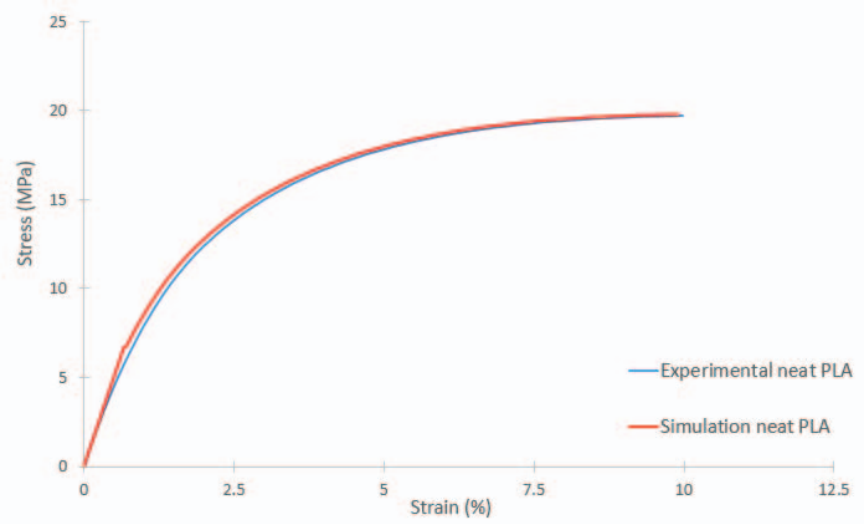

Fig. 9: Stress-strain curves obtained experimentally and via FEA for neat PLA.

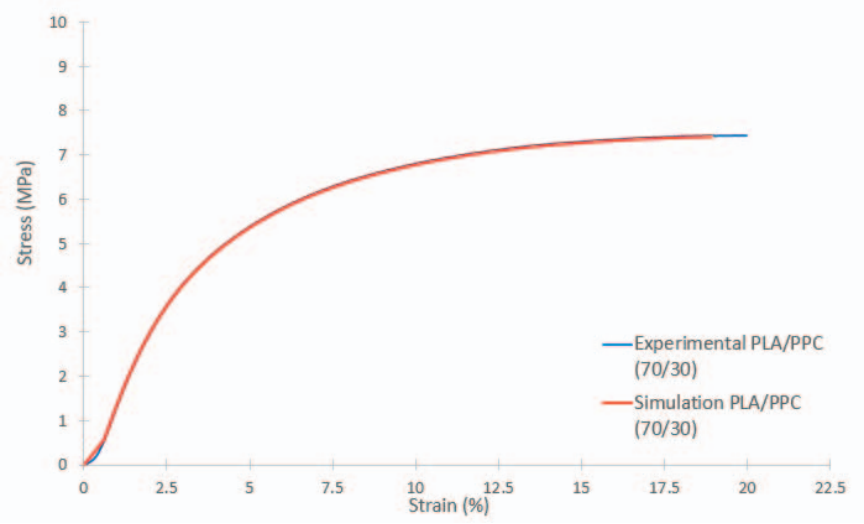

Fig. 10: Stress-strain curves obtained experimentally and via FEA for PLA/PPC.

https://doi.org/10.31436/iiumej.v20i2.1119

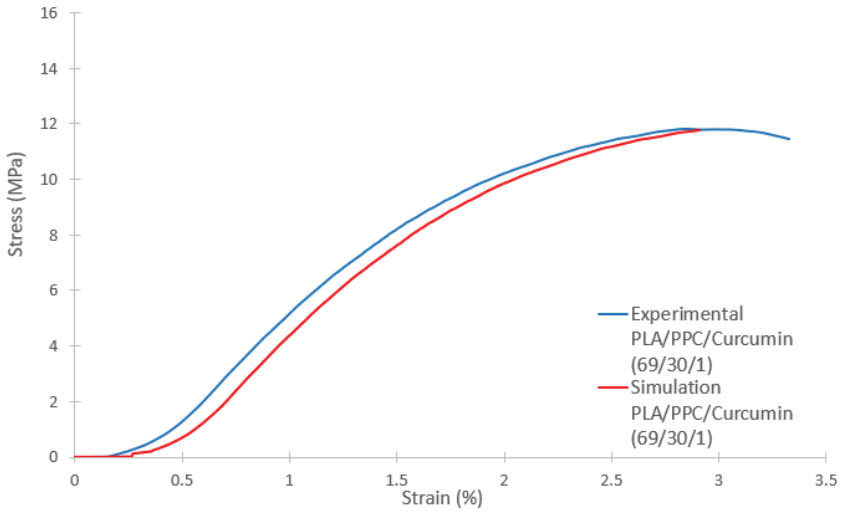

Fig. 11: Stress-strain curves obtained experimentally and via FEA for PLA/PPC/curcumin.

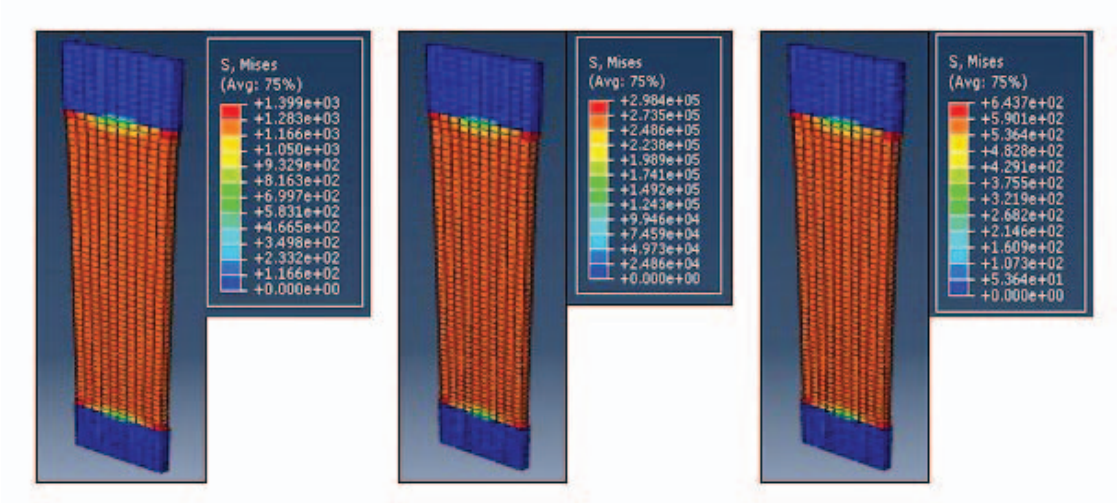

(a) (b) (c)

Fig. 12: Contour plots of computed Von Mises stress along the specimen length for (a) neat PLA, (b) PLA/PPC blend and (c) PLA/PPC/curcumin blend.

Figure 12 shows the distribution of Von Mises stress calculated by the finite element model based on Young's modulus, Poisson ratio, boundary conditions as well as applied load. Similar topography of low to high Von Mises Stress was obtained for all compositions studied. It can be seen from Fig. 13 that the stress distribution is divided into three regions. The first region undergoes no stress since it is the area under grip length, and hence was not deformed. The second region, is noted as the transition phase in which the stress starts to increase. It is also noted that the FE model highlighted the highest Von Mises stress in this transition region between grip and gage length which may indicate the location that possibly initializes the fracture [33]. The model postulated that fracture may occur at either end of the grip length since there were no purposefully designed geometrical flaws such as notches or necking in the simulation model that would trigger localization of the specimen at any desired region. The FE model shows that the addition of PPC into PLA increases the Von Mises stress scale from 1400 MPa to 300 GPa. Whilst the addition of curcumin particles into PLA/PPC blends resulted with reduced Von Mises stress distribution (640 MPa). The values for Young's modulus used for the FE analysis were 936 MPa, 156 MPa and 771 MPa

for PLA, PLA/PPC and PLA/PPC/curcumin respectively. The Young's modulus property influences the stress distribution and hence the elastic deformation of the model [50]. Thus, as the Young's modulus of the sample increases or decreases, correspondingly the upward tensile force respectively causes less or more stress due to the material's resistibility to deformation.

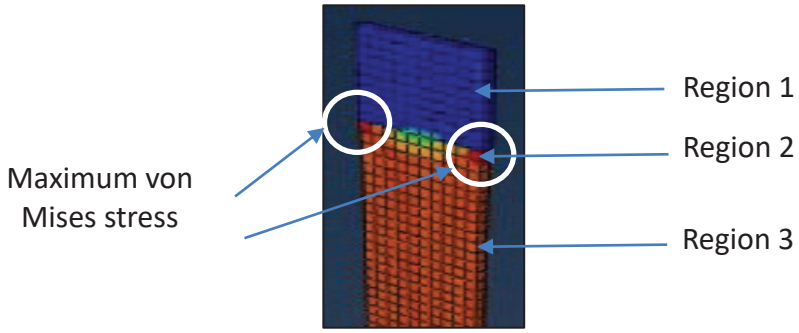

Fig. 13: Identified regions of Von Mises Stress.

4. CONCLUSION

The FTIR analysis illustrated that the chemical interaction, in particular between the carbonyl group (C=O), exists when PPC was added at 30 wt% into PLA. Despite the resultant decrease in strength and modulus, the strain at break increased by 74%. The drop in strength and modulus of PLA/PPC blend was recovered by adding a low weight percentage of curcumin. However, the PLA/PPC/curcumin blend failed at very low tensile strain which shows the increase in the brittle nature of the blend. In light of this observation, it was further confirmed by SEM images that the addition of PPC and curcumin respectively increases its ductility and brittleness. The validation and the excellent agreement between the simulation and experimental results are important indices of the simulated model developed using Abaqus. Hence, this model can be used to predict the performance of complex design components based on PLA/PPC/curcumin blends for biomedical applications.

ACKNOWLEDGEMENT

This work was fully supported by the International Islamic University Malaysia (IIUM), (RIGS17-052-0627). The authors would like to express their deepest gratitude to facilities and technical assistance provided by the International Institute for Halal Research and Training (INHART), IIUM.

REFERENCES

[1] SuPing L, Darrel U. (2009) Degradability of Polymers for Implantable Biomedical Devices. Int J Mol Sci., 9 (10): 4033-4065.
[2] Kaojin W, Satu S, Julian XXZ. (2017) A Mini Review: Shape Memory Polymers for Biomedical Applications. Front Chem Sci Eng., 11(2): 143-153.
[3] Rajendra PP, Sunil UT, Suresh US, Jalinder TT, Abraham JD. (2014) Biomedical Applications of Poly(Lactic Acid). Recent Pat Regen Med., 1(4): 240-251.
[4] Kotiba H, Mosab K, Yang HW, Fawaz D, Young GK. (2015) Properties and Medical Applications of Polylactic Acid: A Review. Polym Lett., 9(5):435–455.
[5] Broz M, David LV, Newell RW. (2003) Structure and Mechanical Properties of Poly(D,L-lactic acid)/Poly(ε-caprolactone) Blends. Biomat., 24:4181-4190.

[6] Erin H, Margaret F. (2014) Increasing Surface Hydrophilicity in Poly(Lactic Acid) Electrospun Fibers by Addition of PLA-β-PEG Co-Polymers. J Eng Fiber Fabr., 9(2):153-164.
[7] Feng-Jiao L, Shui-Dong Z, Ji-Zhao L, Jun-Zhe W. (2015) Effect of Polyethylene Glycol on the Crystallization and Impact Properties of Polylactide-based Blends. Polym. Adv. Technol., 26(5):465-475.
[8] Yanping L, Hanghang W, Zhen W, Qian L, Nan T. (2018) Simultaneous Enhancement of Strength and Toughness of PLA Induced by Miscibility Variation with PVA. Polymers, 10 (10):1178-1191
[9] Ahmed Mohamed E. (2014) The Effect of Additives Interaction on the Miscibility and Crystal Structure of Two Immiscible Biodegradable Polymers. Polimeros, 24(1):9-16.
[10] Yao M, Deng H, Mai F, Wang K, Zhang Q, Chen F, Fu Q. (2011) Modification of Poly(lactic acid)/Poly(Propylene Carbonate) Blends Through Melt Compounding with Maleic Anhydride. Polym Lett., 5(11):937-949.
[11] Sheng-Xue Q, Cui-Xiang Y, Xue-Yang C, Hai-Ping Z, Lifen Z. (2018) Fully Biodegradable Poly(lactic acid)/Poly(propylene carbonate) Shape Memory Materials with Low Recovery Temperature Based on In Situ Compatibilization by Dicumyl Peroxide. Chinese J Polym Sci., 36:783-790.
[12] Mihir S, Ananda Kumar R, Vipul D, Richard AG, Stephen PM. (1997). Biodegradable Polymer Blends of Poly(lactic acid) and Poly(ethylene glycol). J Appl Polym Sci., 66:1495-1505.
[13] Wannapa C, Varaporn T, Jean-Francois P, Pamela P. (2012) Effect of Poly(Vinyl Acetate) on Mechanical Properties and Characteristics of Poly(Lactic Acid)/Natural Rubber Blends. J Polym Environ., 21:450-460.
[14] Baherah B, Yanwei M, Fariba D (2015). Antimicrobial Packaging for Biomedical Applications from a Biodegradable Polymer in Asia Pacific Confederation of Chemical Engineering Congress 2015; Melbourne, Australia.
[15] Youhua T, Xianhong W, Xiaojiang Z, Ji L, Fosong W. (2006) Crosslinkable Poly(propylene carbonate): High-Yield Synthesis and Performance Improvement. J Polym Sci., 44:5329-5336.
[16] Iman M, Ali F, Hesham B, Sean Ryan D, Ali Negahi S, Fariba D. (2016) Biomedical Applications of Biodegradable Polyesters. Polymers, 8(1):20-52.
[17] Dalbir S, Sharma S, Davinder Pal Singh O, Idress Ahmed W. (2010) Effect of Extraction Parameters on Curcumin Yield from Turmeric. J Food Sci. Technol., 47(3):300-304.
[18] David E R, Biotechnology 2, Global Prospects, Florida: CRC Press, 2011.
[19] Bharat A, Bokyung S. (2009) Pharmacological Basis for the Role of Curcumin in Chronic Diseases: An Age-old Spice with Modern Targets. Trends Pharmacol Sci., 30(2):85-94.
[20] Sahdeo P, Amit Tyagi K, Bharat A. (2014) Recent Developments in Delivery, Bioavailability, Absorption and Metabolism of Curcumin: the Golden Pigment from Golden Spice. Cancer Res. Treat., 46(1): 2-18.
[21] Nithya R, Tamil Selvan N, Sheeja R. (2015) Preparation and Characterization of Electrospun Curcumin Loaded Poly(2-hydroxyethyl methacrylate) Nanofiber-a Biomaterial for Multidrug Resistant Organisms. J Biomed Mater Res., 103(1):16-24.
[22] Xia F, Chun Z, Dong-Bu L, Jun Y, Hua-Ping L. (2013) The Clinical Applications of Curcumin: Current State and the Future. Curr Pharm Des., 19:11-13.
[23] Xiao-Zhu S, Gareth R W, Xiao-xiao H, Li-Min Z. (2013) Electrospun Curcumin-loaded Fibers with Potential Biomedical Applications. Carbo Polym., 94:147-153.
[24] Thuy Thi T N, Chiranjit G, Seong Gu H, Tran Dai L, Jun Seo P. (2013) Characteristics of Curcumin –loaded Poly(lactic) Nanofibers for Wound Healing. J Mater Sci, 48:7125-7133
[25] Bhaarathi D, Saraswathy N, Ramasamy M, Ponnusamy S, Palanisamy V, Sukumar V, Venugopal R. (2013) Electrospinning of Curcumin Loaded Chitosan/Poly (lactic acid) Nanofilm and Evaluation of its Medicinal Characteristics. Front Mat Sci., 7(4):350-361.
[26] Heni R, Yulia Lie Y, Annisa R, Noboyuki M. (2016) Curcumin-loaded PLA Nanoparticles: Formulation and Physical Evaluation. Sci Pharma., 84(1):191-202.

[27] Li-mei J, Yi-chun Z, Yongli H. (2010) Elastic-plastic Properties of Thin Film on Elastic-plastic Substrates Characterized by Nanoindentation Test. T Nonferr Metal Soc., 20(12):2345-2349.
[28] Senthil E, Ashley Kelley J, Jorgen B, Virginia L G (2011). Material Modeling of Polylactide, in Simulia Customer Conference, Barcelona, Spain, 2011.
[29] Harpen L, Ahmed I, Felfel RM, Qian C. (2012) Finite Element Modelling of the Flexural Performance of Resorbable Phosphate Glass Fibre Reinforced PLA Composite Bone Plates. J Mech Behav Biomed Mater., 15:13-23.
[30] Anna B, Susana PF, Jose-Ramon S, Wang W, Peter EM. (2015) Computational Bench Testing to Evaluate the Short-Term Mechanical Performance of a Polymeric Stent. Cardio Eng Tech., 6(4):519-532.
[31] Andrea Costa V, Antonio T. M, Rui Miranda G, Volnei T. (2011) Material Model Proposal for Biodegradable Materials. Procedia Eng., 10:1597-1602.
[32] Joao Silve S, James E M, Kumbakonan RR. (2008) Constitutive Framework for Biodegradable Polymers with Applications to Biodegradable Stents. Asaio J., 54(3): 295-301.
[33] Link RE, Garrell MG, Albert S, Edgar LC, Ronald S. (2003) Finite-Element Analysis of Stress Concentration in ASTM D 638 Tension Specimens. J Test Eval., 31(1):1-6.
[34] Mayank N, Anurag D, Misra R K, Harlal Singh M. (2014) Tensile Test Simulation of CFRP Test Specimen Using Finite Elements. Procedia Mat Sci., 5:267-273.
[35] Jonathan T, Jose C, Justin K, Ali PG. (2015). Mechanical Property Optimization of FDM PLA in Shear with Multiple Objectives. JOM., 67(5):1183-1193.
[36] Shuwen P, Xiuyan W, Lisong D. (2005) Special Interaction Between Poly (propylene carbonate) and Corn Starch. Polymer Composite, 26:37-41.
[37] Kurniawan Y, Yohanes Aris P, Setyo P, Bruce A W, Hadi Karia P, Titi Candra S. (2015) Infrared and Raman Studies on Polylactide Acid and Polyethylene Glycol-400 Blend. in AIP Conference Proceedings of the Third International Conference on Advanced Materials Science and Technology (ICAMST 2015): 6-7 Oct 2015; Semarang. Edited by Sutikno, Khairurrijal, Heru Susanto, Risa Suryana, Kuwat Triyana and Markusdiantoro, AIP Publishing; pp 0201011-0201016.
[38] Xiaofei M, Jiugao Y, Ning W. (2006) Compatibility Characterization of Poly(lactic acid)/Poly(propylene carbonate) Blends. J Polym Sci Pt B., 44: 94-101.
[39] Rosana Aparecida da S, Mateus Ferreira de S, Daniela O, Evandro B. (2016) Preparation of Curcumin-loaded Nanoparticles and Determination of the Antioxidant Potential of Curcumin after Encapsulation. Polimeros, 26(3):207-214.
[40] Harshal Ashok P, Karde M, Mundle N, Jadhav P. (2014) Phytochemical Evaluation and Curcumin Content Determination of Turmeric Rhizomes Collected From Bhandara District of Maharashtra (India). Med. Chem., 4(8):588-591.
[41] Duong Quang L, Trang M, Thi Thu T N, Thi Ngoan N, Thi Cham B, Nguyen Hai B, Thi Bich H P, Tran Dai L, Jun Seo P. (2012) A Novel Nanofiber Cur-loaded Polylactic Acid Constructed by Electrospinning. Adv Nat Sci-Nanosci., 3:1-5.
[42] Yan C, Jie L, Yanna F, Hongbo W. (2010) Preparation and Characterization of Electrospinning PLA/Curcumin Composite Membranes. Fib Polym., 11(8):1128–1131.
[43] Wei Z, Rongyuan C, Guizhen Z, Haichen Z. (2016) Mechanical, Thermal and Rheological Properties and Morphology of Poly (lactic Acid)/Poly (propylene Carbonate) Blends Prepared by Vane Extruder. Polym Adv Technol,. 27(11): 1430-1437.
[44] Cuixiang Y, Ruirui Z, Haiyue W. (2018) The Mechanical Property of PLA/PPC Blends. Int J Trend Res Dev., 5(2):206-208.
[45] Qirui S, Tizazu M, Manjusri M, Amar M. (2016) Novel Biodegradable Cast Film from Carbon Dioxide Based Copolymer and Poly(Lactic Acid). J Polyms Environ., 24(1):23-36.
[46] Nurdina Abdul K, Mariatti J, Samayamutthirian P. (2009) Effect of Single-Mineral Filler and Hybrid-Mineral Filler Additives on the Properties of Polypropylene Composites. J Vinyl Addit Techn., 15(1):20-28.

[47] Sharifah Imihezri S S, Qairol A A B, Noor Azlina H, Nor Khairusshima MK. (2017) Thermal, Structural and Mechanical Properties of Melt Drawn Curloaded Poly(lactic acid) Fibers. Procedia Eng., 184:544 - 551.
[48] Zhao W, Xiangling L, Min Z, Wei Y, Mingbo Y. (2017). Synthesis of an Efficient Processing Modifier Silica-g-poly (lactic acid)/Poly (propylene carbonate) and its Behavior for Poly (lactic acid)/poly (propylene carbonate) Blends. Ind Eng Chem Res., 56 (49):14704-14715.
[49] Baki H. (2014). The Properties of PLA/Oxidized Soybean Oil Polymer Blends. J Polym Environ., 22(2):200-208.
[50] Yongtao W, Liming K, Sizhuo S, Yuxing D, Zhong G, Zhirui Y, Qigang Z. (2013) Finite Element Analysis on Von Mises Stress Distributions of Si DSP. Mater Sci Semicond Process., 16(1):165-170.